SCIENTIFIC REPORTS

OPEN

SUBJECT AREAS:
QUANTUM PHYSICS
MAGNETIC MATERIALS AND DEVICES
CONDENSED MATTER PHYSICS
STATISTICAL PHYSICS, THERMODYNAMICS AND NONLINEAR DYNAMICS

Received
25 April 2012

Accepted
16 May 2012

Published
30 May 2012

Correspondence and requests for materials should be addressed to X.Y.P. (xypan@aphy.iphy.ac.cn) or R.B.L. (rbliu@phy.cuhk.edu.hk).

* Current address: 3rd Physics Institute and Research Center SCoPE, University of Stuttgart, 70569 Stuttgart, Germany.

Controllable effects of quantum fluctuations on spin free-induction decay at room temperature

Gang-Qin Liu[1], Xin-Yu Pan[1], Zhan-Feng Jiang[2], Nan Zhao[2]* & Ren-Bao Liu[2]

[1]Beijing National Laboratory for Condensed Matter Physics, Institute of Physics, Chinese Academy of Sciences, Beijing 100190, China, [2]Department of Physics and Centre for Quantum Coherence, The Chinese University of Hong Hong, Shatin, New Territories, Hong Kong, China.

Fluctuations of local fields cause decoherence of quantum objects. Usually at high temperatures, thermal noises are much stronger than quantum fluctuations unless the thermal effects are suppressed by certain techniques such as spin echo. Here we report the discovery of strong quantum-fluctuation effects of nuclear spin baths on free-induction decay of single electron spins in solids at room temperature. We find that the competition between the quantum and thermal fluctuations is controllable by an external magnetic field. These findings are based on Ramsey interference measurement of single nitrogen-vacancy center spins in diamond and numerical simulation of the decoherence, which are in excellent agreement.

Quantum systems lose their coherence when subjected to fluctuations of the local fields. Such decoherence phenomena are a fundamental effect in quantum physics[1–3] and a critical issue in quantum technologies[4–11]. The local field can have both thermal and quantum fluctuations. At finite temperature[12], the environment (bath) is in a thermal distribution, which can be formulated as a density matrix $\rho_E = \Sigma_J p_J |J\rangle\langle J|$ with p_J denoting the probability for the bath in the state $|J\rangle$. If the local field operator b commutes with the total bath Hamiltonian H_E, the state $|J\rangle$ can be chosen as an eigenstate of the local field with eigenvalue b_J. Therefore the thermal distribution induces the local field fluctuation $\sigma^{th} = \sqrt{\sum_J p_J b_J^2 - \left(\sum_J p_J b_J\right)^2}$, which is called thermal fluctuation. In general, the local field operator b does not commute with the total Hamiltonian of the bath H_E. Thus a certain eigenstate $|b_0\rangle$ of b is not an eigenstate of the total Hamiltonian and will evolve to a superposition of different eigenstates of b at a later time t, i.e., $|b_0(t)\rangle = \Sigma_J C_J |b_J\rangle$. Then a measurement of the local field at a later time would yield random distribution, causing quantum fluctuation of the local field $\sigma^q = \sqrt{\sum_J |C_J|^2 b_J^2 - \left(\sum_J |C_J|^2 b_J\right)^2}$[13]. The quantum fluctuation is directly related to the internal interactions within the baths. Thus the study of quantum fluctuation and singling it out of the thermal fluctuation are not only of fundamental interest for understanding decoherence in quantum physics but also of interest for identifying microscopic structures (such as nuclear spin configurations) in quantum technologies (such as nano-magnetometry and quantum computing via central spins).

Usually at high-temperatures (as compared with transition energies of the bath), the thermal fluctuations are much stronger than the quantum fluctuations. It has been well known that spin-echo or dynamical decoupling control in magnetic resonance spectroscopy[14–17] can largely suppress the decoherence effects of thermal fluctuations and single out the effects of quantum fluctuations. The quantum control over the central spins as in spin echo, however, may also fundamentally modify the dynamics of the baths via the central spin-bath interaction[18]. While the control of bath dynamics in spin echo is of great interest in its own right and has been extensively studied, it is highly desirable to have quantum fluctuation examined in free evolution and to study the interplay between the thermal and quantum fluctuation in their co-existence.

In this paper, we show that in the case of strong system-bath coupling (as compared with the internal Hamiltonian of the bath), the quantum fluctuation can be comparable to the thermal fluctuation. The quantum fluctuations can induce notable effects on free-induction decay of the central spin coherence even at room temperature (which can be regarded as infinite for the nuclear spin baths considered here). The competition between the thermal and quantum fluctuations can be controlled by an external magnetic field, indicated by crossover between Gaussian and non-Gaussian decoherence accompanied by decoherence time variation. In

addition to revealing a surprising aspect of the quantum nature of nuclear spin baths, the effect can be used to identify optimal physical systems and parameter ranges for quantum control over a few nuclear spins via a central electron spin. Such control is relevant to quantum computing[6,7] and nano-magnetometry[8–11].

Results

Theoretical background and model. The model system in this study is a nitrogen-vacancy center (NVC) electron spin coupled to a bath of ^{13}C nuclear spins in diamond. This system has promising applications in quantum computing[6,7] and nano-magnetometry[8–11]. The hyperfine interaction between the NVC spin and the bath spins is essentially dipolar and therefore anisotropic. Due to the anisotropy of the interaction, the hyperfine field on a nuclear spin is in general not parallel or antiparallel to the external magnetic field and therefore the local Overhauser field b (as a bath operator) does not commute with the Zeeman energy of the bath. This induces strong quantum fluctuations, when the external field is not too strong or too weak. The model system is representative of a large class of central spin decoherence problems in which a central spin (such as associated with impurities or defects in solids) has anisotropic dipolar interaction with bath spins[19].

The NVC has a spin-1, which has a zero-field splitting $\Delta \approx 2.87$ GHz between the states $|0\rangle$ and $|\pm 1\rangle$, quantized along the z-axis (the nitrogen-vacancy axis). Since the NVC spin splitting is much greater than the hyperfine interaction with the ^{13}C spins, the center spin flip due to the Overhauser field can be safely neglected[7]. We only need to consider the z-component of the local field fluctuation, $b_z = \Sigma_j \mathbf{A}_j \cdot \mathbf{I}_j$, where $\mathbf{A}_j$ is the dipolar coupling coefficients for the jth nuclear spin $\mathbf{I}_j$. The local field b_z is a quantum operator of the bath. Within the timescales considered in this paper, the interaction between the ^{13}C nuclear spins, which has strength less than a few kHz[20,22], can be neglected. The only internal Hamiltonian of the bath is the Zeeman energy under an external magnetic field, $H_E = \Sigma_j \gamma_C \mathbf{I}_j \cdot \mathbf{B}$, where $\gamma_C = 6.73\times10^7$ T^{-1}s^{-1} is the gyromagnetic ratio of ^{13}C. To be specific, the magnetic field $\mathbf{B}$ is applied along the z axis in this paper. The Hamiltonian of the NVC spin and the bath can be written as[20,22]

$$H = \Delta S_z^2 + (\gamma_e B + b_z) S_z + H_E, \qquad (1)$$

where $\gamma_e = 1.76\times10^{11}$ T^{-1}s^{-1} is the electron gyromagnetic ratio, and S_z is the NVC spin operator along the z-axis.

Thermal and quantum fluctuations. At room temperature, the nuclear spins are totally unpolarized. Thus the bath can be described by a density matrix $\rho_E = 2^{-N} I$, with N being the number of ^{13}C included in the bath, and I is a unity matrix of dimension 2^N. When the bath contains a large number of nuclear spins (for example, $N > 10$), the local Overhauser field has a Gaussian distribution with width[12]

$$\sigma^{th} = \sqrt{\langle b_z^2\rangle - \langle b_z\rangle^2} = \frac{1}{2}\left(\sum_j A_j^2\right)^{1/2}, \qquad (2)$$

where $\langle b_z^2\rangle \equiv \mathrm{Tr}[\rho_E b_z^2]$ and $\langle b_z\rangle \equiv \mathrm{Tr}[\rho_E b_z]$. This so-called inhomogeneous broadening would cause a Gaussian decay of the NVC spin coherence, $e^{-(t/T_2^*)^2}$ with the dephasing time $T_2^* = \sqrt{2}/\sigma^{th}$.

The quantum fluctuation of the local field b_z arises from the fact that in general $[b_z, H_E] \neq 0$, especially when the nuclear Zeeman energy is comparable to the hyperfine coupling $\gamma_C B \sim A_j$[22]. In the weak field case $\gamma_C B \ll A_j$, the effect of the quantum fluctuations would be negligible. In the strong field case $\gamma_C B \gg A_j$, the quantum fluctuation would also be suppressed, since the nuclear spin flips due to the off-diagonal hyperfine interaction (components of $\mathbf{A}_j$ perpendicular to the z-axis) would be suppressed by the large Zeeman energy cost. In addition, the local field fluctuation under a strong external field should contain only the diagonal part, i.e., in equation (2) for the inhomogeneous broadening, $\mathbf{A}_j$ should be replaced with the z-component A_j^z. Therefore, we expect the dephasing time in the strong field limit is longer than that in the weak field limit. Such suppression of central spin dephasing by a strong magnetic field has indeed been observed previously for NVC spins in electron spin baths[21]. In the transition regime, the quantum fluctuation effect would be important, and the dephasing would be in general non-Gaussian. Such features of NVC center spin dephasing have been noticed previously in numerical simulations[22].

Experimental procedure. We use optically detected magnetic resonance (ODMR)[23] to measure the Ramsey interference (see Methods for details) of single NVC spins in a high-purity type-IIa single-crystal diamond (with nitrogen density $\ll$1 ppm)[7]. All the experiments are performed at room temperature. Single NVC's in diamond are addressed by a home-built confocal microscope system [see Fig. 1(a) for a typical fluorescence image of the single NVC's]. An external magnetic field is applied along the z-axis. The field strength is tunable from 0 to 305 Gauss. Under a weak field [10.3 Gauss as shown in Fig. 1(c)], the two NVC spin transitions $|0\rangle \leftrightarrow |\pm 1\rangle$ are well resolved in spectrum. Furthermore, due to the hyperfine coupling to the ^{14}N nuclear spin, each NVC spin transition is split into three lines corresponding to the three states of the ^{14}N nuclear spin-1[7], which are resolved by pulse-ODMR[24] measurement [see Fig. 1 (d) for the $|0\rangle \leftrightarrow |-1\rangle$ transition]. Fig. 1(b) shows the high-fidelity rotation of the NVC spin under a microwave pulse of different durations.

Experimental results. Typical Ramsey interference signals of a single NVC spin are shown in Fig. 2. The oscillation is due to the beating between different transition lines corresponding to the three ^{14}N spin states[7]. Each of the transition contributes 1/3 signal, and the frequency of the signal is equal to the microwave detuning. We

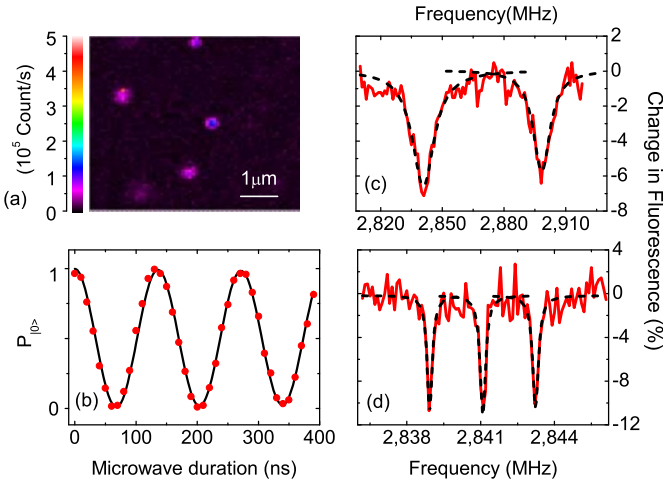

Figure 1 | Optically detected magnetic resonance of single nitrogen-vacancy centers in a type-IIa diamond. (a) A fluorescence image of single NVC's. (b) Rabi oscillation of an NVC spin driven by a microwave pulse with the same strength as used in the Ramsey signal measurement. (c) Continuous-wave ODMR spectrum of an NVC spin, measured with a relatively strong microwave field (such that different lines due to different ^{14}N nuclear spin states are not resolved). The two peaks (fitted with Lorentzian lineshapes in dashed lines) correspond to the transitions $|0\rangle \leftrightarrow |\pm 1\rangle$. (d) Pulse ODMR spectrum near the $|0\rangle \leftrightarrow |-1\rangle$ transition of an NVC spin, measured with a relatively weak microwave field (such that different lines due to different ^{14}N nuclear spin states are resolved, fitted with Gaussian lineshapes in dashed lines). The magnetic field is 10.3 Gauss in the measurement.

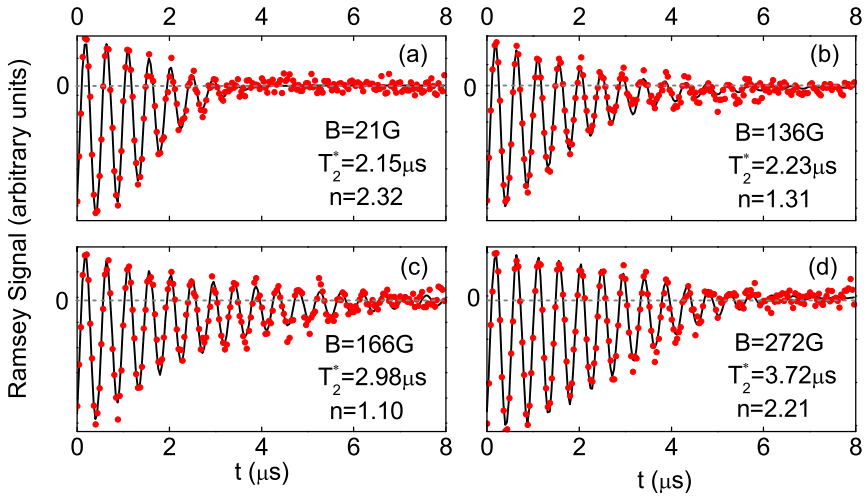

Figure 2 | Typical Ramsey signals of an NVC as functions of time under various magnetic field strengths. (a) B = 21 Gauss, (b) B = 136 Gauss, (c) B = 166 Gauss, and (d) B = 272 Gauss. The red symbols are measured results, and the black lines are fitting with equation (3).

tune the frequency of the microwave pulse to match the central transition, so there is 1/3 signal without oscillation, and the remaining 2/3 signal oscillates at a frequency equal to the microwave detuning, which is the hyperfine coupling $A_{^{14}N}$ to the ^{14}N nuclear spin. As shown in Fig. 2, The spin coherence represented by the fluorescence change as a function of time, after subtraction of the background photon counting, is well fitted with the formula

$$S = Ce^{-(t/T_2^*)^n}\left[\frac{1}{3}+\frac{2}{3}\cos(A_{^{14}N}t+\phi)\right], \qquad (3)$$

in which T_2^* gives the spin dephasing time, and the exponential index n characterizes the non-Gaussian nature of the dephasing (n = 2 corresponding to the Gaussian dephasing case).

The magnetic field strongly affects the dephasing behavior. In the weak magnetic field region [Fig. 2(a)], T_2^* is about 2 μs and the exponential index $n \approx 2$, corresponding to the Gaussian dephasing case. The decay behavior becomes non-Gaussian when the external magnetic field increases. The strongest non-Gaussian behavior appears at B = 166 Gauss, where n = 1.1. The Gaussian decay appears again when the magnetic field reaches the strong region (Fig. 2(d)), with a dephasing time ($T_2^* = 3.72$ μs at 272 Gauss) longer than in the weak field region.

Other NVC's have similar dephasing behaviors, but the dephasing times and transition regions for different NVC's are notably different. The Ramsey interference signals of three different NVC's (labeled A, B and C) are shown in Fig. 3 (a–c). Among our measurements, the longest dephasing time reaches 7.53 μs (Fig. 3(a)), and the shortest dephasing times is just 0.83 μs (Fig. 3(c)).

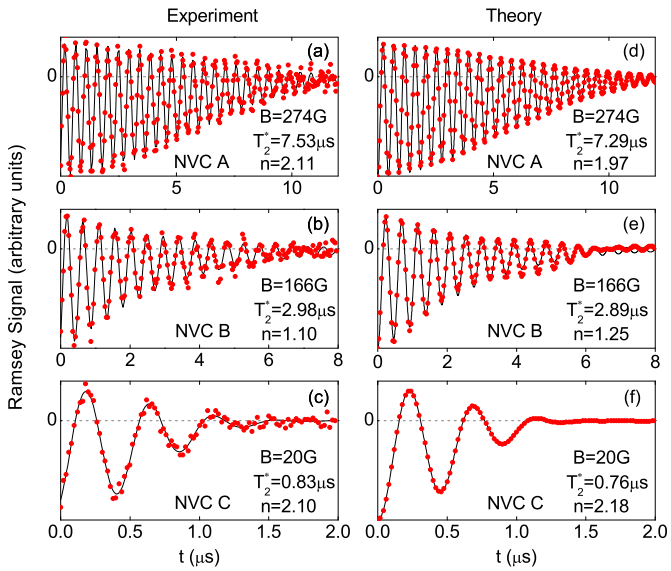

Figure 3 | Comparison between numerical and experimental results of Ramsey signals. (a), (b), and (c) in turn show three typical cases of experimentally measured Ramsey signals as functions of time for three NVC's A, B, and C under different magnetic fields. (d), (e), and (f) are numerical simulations corresponding to (a), (b), and (c) in turn. The red symbols are measured or calculated results, and the black lines are fitting with equation (3).

Discussions

Figure 4 shows the spin dephasing time T_2^* and the exponential decay index n as functions of the external magnetic field strength for three

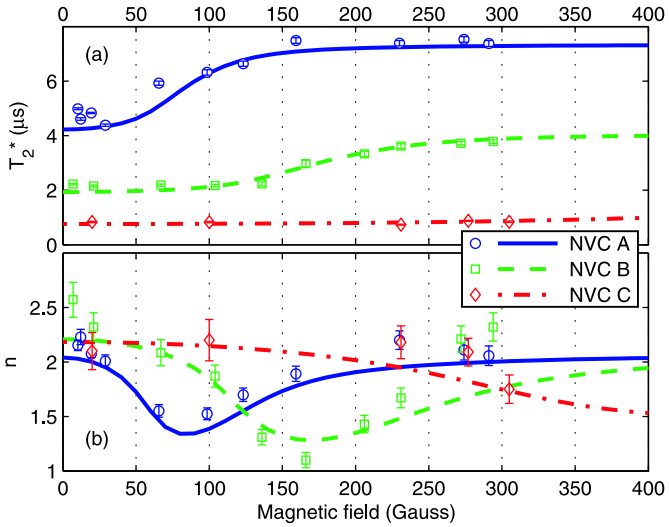

Figure 4 | Dependence on the magnetic field strength of the NVC spin dephasing. (a) the dephasing time T_2^*, and (b) the exponential decay index n, for three NVC's (A, B, and C). Experimental data are shown in circle, square, and diamond symbols with error bars, and numerical data are shown in solid, dashed, and dash-dotted lines.

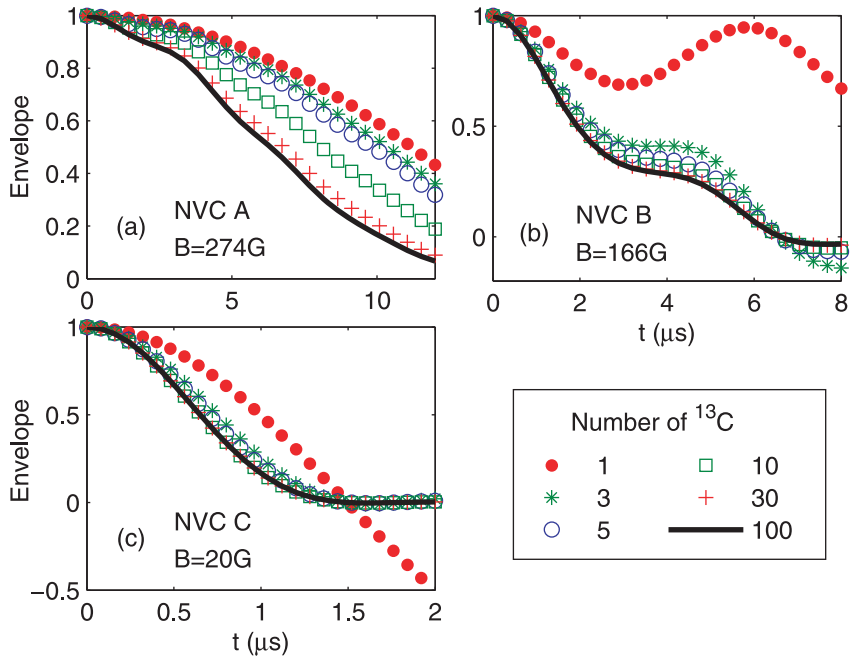

Figure 5 | Decay envelopes of the calculated Ramsey signals for various numbers of nearest ^{13}C nuclear spins included in the bath. (a), (b), and (c) show results calculated under the conditions corresponding to Fig. 3(d), (e), and (f) in turn. The number of nuclear spins is $N = 1, 3, 5, 10, 30$, and 100 for filled circles, stars, open circles, open squares, crosses, and solid lines in turn.

different NVC's. The increasing of the dephasing time with the magnetic field strength and the non-Gaussian decay associated with the dephasing time rising demonstrate the competition between the thermal fluctuations of the local fields and the quantum fluctuations. Since the ^{13}C atoms (with abundance of 1.1%) are randomly located around the NVC's, the dephasing time T_2^* presents a random distribution depending on the ^{13}C position configurations[22]. An NVC with longer dephasing time should have ^{13}C atoms located farther away from the center with weaker hyperfine interaction (as the hyperfine interaction is dipolar and decays rapidly with distance from the center). Therefore, we expect that the quantum fluctuations for NVC's with longer dephasing times start to take effect at lower magnetic field. This is indeed confirmed by the three sets of data representing NVC's with long, intermediate, and short dephasing time (NVC A, B and C in turn).

To further confirm the physical picture of the quantum-thermal fluctuation crossover, we carry out numerical simulations of the Ramsey signals with no fitting parameters. Since the positions of the ^{13}C atoms are not determined and the dephasing time depends on the positions of the nuclear spins, we randomly choose the spatial configurations such that the dephasing times at zero field are close to the experimental values at the lowest field. As shown in Fig. 3 (d–f), the calculated results are well fitted with equation (3). The dephasing time and the exponential decay index obtained from the numerical results are in excellent agreement with the experimental data (see Fig. 4).

Figure 5 shows the contributions of nuclear spins at different distances to the NVC spin dephasing. The nearest few ^{13}C nuclear spins already contribute the major part of the local field fluctuations. A close examination of the ^{13}C positions in different configurations reveals that the average hyperfine coupling constants for the nearest 10, 5, and 3 nuclear spins (which contribute the major part of the dephasing) for NVC A, B, and C are $\bar{A} \approx 0.16$, 0.51, and 1.7 μs^{-1} in turn. Correspondingly, the quantum fluctuations should start to take effect at magnetic field strength $B \sim \bar{A}/\gamma_C \approx 24$, 76, and 260 Gauss for NVC A, B, and C in turn. This is indeed consistent with the experimental observation shown in Fig. 4. Figure 5 (b) presents some pronounced oscillation features, as also seen in Fig. 3 (b) and (e). Such oscillations are due to a few ^{13}C nuclei located relatively close to the NVCs. The details of the oscillations, however, depend on the specific positions of the nuclei. Such features, after careful analysis, may be employed to identify a few ^{13}C nuclei near the NVC, which is useful in atomic scale magnetometry[10].

Methods

Ramsey interference measurement scheme. The single NVC spin is first initialized to the state $|0\rangle$ by optical pumping with a 532 nm laser pulse of 3.5 μs duration. Then a $\pi/2$ microwave pulse excites the NVC spin to the superposition state $(|0\rangle + |-1\rangle)/\sqrt{2}$. The pulse is tuned resonant with the central line (corresponding to the ^{14}N spin state $|0\rangle_{^{14}N}$) of the $|0\rangle \leftrightarrow |-1\rangle$ transition for each magnetic field. The pulse duration [34 ns, corresponding to $\pi/2$ rotation in Fig. 1(b)] is chosen long enough to avoid the $|0\rangle \leftrightarrow |+1\rangle$ transition and short enough to spectrally cover all the three hyperfine lines corresponding to different ^{14}N nuclear spin states. After the first microwave pulse, the spin is left to freely precess about the magnetic field with dephasing. After a delay time t, a second $\pi/2$ microwave pulse is applied to convert the spin coherence to population in the state $|-1\rangle$. The fluorescence of the NVC, which is about 30% weaker when the spin is in $|-\rangle$ than it is when the spin is in $|0\rangle$, is detected by photon counting under illumination of a 532 nm laser of 0.35 μs duration. Each measurement (for a certain B field and delay time t) is typically repeated 0.4 ~ 1 million times to accumulate sufficient signal-to-noise ratio.

Calculation of the signals. The calculation is done with only single nuclear spin dynamics taken into account (the interactions between nuclear spins are neglected since they are not relevant in the timescales considered in this paper), which is an exactly solvable problem. The Ramsey signal is given by[20,22]

$$S = \sum_{m=0,\pm 1} e^{imA_{^{14}N}t} \prod_{n=1}^{N} \mathrm{Tr}\left[e^{i\gamma_C B I_j^z t} e^{iA_j \cdot I_j t - i\gamma_C B I_j^z t}\right]. \quad (4)$$

In the simulations, the nearest 500 nuclear spins are included ($N = 500$), which produces well converged results.

1. Zurek, W. H. Decoherence and the transition from quantum to classical. *Phys. Today* **44**, 36–44 (1991).
2. Joos, E. *et al. Decoherence and the Appearance of a Classical World in Quantum Theory* (Springer, New York, 2003) 2nd ed.
3. Schlosshauer, M. Decoherence, the measurement problem, and interpretations of quantum mechanics. *Rev. Mod. Phys.* **76**, 1267–1303 (2004)
4. Clarke, J. & Wilhelm, F. K. Superconducting quantum bits. *Nature* **453**, 1031–1042 (2008).

5. Ladd, T. D. *et al*. Quantum computers. *Nature* **464**, 45–53 (2010).
6. Wrachtrup, J. & Jelezko, F. Processing quantum information in diamond. *J.Phys. - Cond. Mat.* **18**, S807–S824 (2006).
7. Childress, L. *et al*. Coherent dynamics of coupled electron and nuclear spin qubits in diamond. *Science* **314**, 281–285 (2006).
8. Maze, J. R. *et al*. Nanoscale magnetic sensing with an individual electronic spin in diamond. *Nature* **455**, 644–647 (2008).
9. Balasubramanian, G. *et al*. Nanoscale imaging magnetometry with diamond spins under ambient conditions. *Nature* **455**, 648–651 (2008).
10. Zhao, N., Hu, J. L., Ho, S.-W., Zhao, N., Hu, J. L., Ho, S.-W., Wan, J. T. K. & Liu, R. B. Atomic-scale magnetometry of distant nuclear spin clusters via nitrogen-vacancy spin in diamond. *Nature Nanotech.* **6**, 242–246 (2011).
11. Grinolds, M. S. *et al*. Quantum control of proximal spins using nanoscale magnetic resonance imaging. *Nature Phys.* **7**, 687–692 (2011).
12. Merkulov, I. A., Efros, A. L. & Rosen, M. Electron spin relaxation by nuclei in semiconductor quantum dots. *Phys. Rev. B* **65**, 205309 (2002).
13. Zhao, N., Wang, Z. Y. & Liu, R. B. Anomalous Decoherence Effect in a Quantum Bath. *Phys. Rev. Lett.* **106**, 217205 (2011).
14. Hahn, E. L. Spin echoes. *Phys. Rev.* **80**, 580–594 (1950).
15. Du, J. F. *et al*. Preserving electron spin coherence in solids by optimal dynamical decoupling. *Nature* **461**, 1265–1268 (2009).
16. Ryan, C. A., Hodges, J. S. & Cory, D. G. Robust decoupling techniques to extend quantum coherence in diamond. *Phys. Rev. Lett.* **105**, 200402 (2010).
17. Huang, P. *et al*. Observation of an anomalous decoherence effect in a quantum bath at room temperature. *Nature Communications* **2**, 570 (2011).
18. Yao, W., Liu, R. B. & Sham, L. J. Restoring lost coherence to a slow interacting mesoscopic spin bath. *Phys. Rev. Lett.* **98**, 077602 (2007).
19. Dobrovitski, V. V., Feiguin, A. E., Hanson, R. & Awschalom, D. D. Decay of Rabi oscillations by dipolar-coupled dynamical spin environments. *Phys. Rev. Lett.* **102**, 237601 (2009).
20. Maze, J. R., Taylor, J. M. & Lukin, M. D. Electron spin decoherence of single nitrogen-vacancy defects in diamond. *Phys. Rev. B* **78**, 094303 (2008).
21. Hanson, R., Dobrovitski, V. V., Feiguin, A. E., Gywat, O. & Awschalom, D. D. Coherent Dynamics of a single spin interacting with an adjustable spin bath. *Science* **320**, 352–355 (2008).
22. Zhao, N., Ho, S. W. & Liu, R. B. Decoherence and dynamical decoupling control of nitrogen-vacancy center electron spins in nuclear spin baths. *Phys. Rev. B* **85**, 115303 (2012).
23. Gruber, A. *et al*. Scanning Confocal Optical Microscopy and Magnetic Resonance on Single Defect Centers. *Science* **276**, 2012–2014 (1997).
24. Dréau, A. *et al*. Avoiding power broadening in optically detected magnetic resonance of single NV defects for enhanced dc magnetic field sensitivity. *Phys. Rev. B* **84**, 195204 (2011).

Acknowledgement

This work was supported by National Basic Research Program of China (973 Program project No. 2009CB929103), the National Natural Science Foundation of China Grants 10974251 and 11028510, Hong Kong Research Grants Council/General Research Fund CUHK402208 and CUHK402410, and The Chinese University of Hong Kong Focused Investments Scheme.

Author Contributions

X.Y.P. and R.-B.L designed the project. X.Y.P. and G.Q.L. performed the experiment. Z.F.J and R.B.L. performed the theoretical study. R.-B.L. wrote the paper. All authors analyzed the data and commented on the manuscript.

Additional information

Competing financial interests: The authors declare no competing financial interests.

How to cite this article: Liu, G., Pan, X., Jiang, Z., Zhao, N. & Liu, R. Controllable effects of quantum fluctuations on spin free-induction decay at room temperature. *Sci. Rep.* **2**, 432; DOI:10.1038/srep00432 (2012).